The Evaluation of Composite Energy Absorbers for use in UAM eVTOL Vehicle Impact Attenuation

Justin Littell
Justin.D.Littell@nasa.gov
Research Aerospace Engineer
NASA Langley Research Center
Hampton VA, 23681

Jacob Putnam
Jacob.B.Putnam@nasa.gov
Research Aerospace Engineer
NASA Langley Research Center
Hampton VA, 23681

Robin Hardy
Robin.C.Hardy@nasa.gov
Research Aerospace Engineer
NASA Langley Research Center
Hampton VA, 23681

ABSTRACT

The demand for new personal air-taxi services is leading to the development of lightweight Vertical Take-off and Landing (eVTOL) vehicles with electric propulsion for the Urban Air Mobility (UAM) industry. Manufacturers (OEMs) are considering many different designs to develop a vehicle that is able to take-off, cruise, and land autonomously with seating arrangements ranging between 2 and 15 passengers. It is unclear at present how the eventual market will mature; however, one of the common design characteristics noted by many of the OEMs is the use of advanced materials such as composites.

A test and analysis program was initiated at NASA Langley Research Center (LaRC) in 2018 to evaluate the impact attenuation capabilities of various composite material systems with the goal of eventual implementation into an eVTOL vehicle. A series of 3-inch diameter by 6-inch length tubular specimens were fabricated from different material systems which included both traditional carbon and hybrid woven layers of fibers. Additionally, a subset of specimens were filled with closed-cell polyisocyanurate foam to help both with stabilization and crush response. The ultimate goal of the test program was to design a specimen capable of limiting the sustained crush acceleration to 20 g through a stable crush progression. After a series of material tests, these specimens were evaluated under both static and dynamic conditions for impact energy attenuation characteristics and crush stability.

Additionally, a series of simulation models were developed in parallel to the test efforts. It is anticipated that the models developed using the component level test efforts can be used to help guide the development of a design for use in full-scale eVTOL vehicle applications.

Introduction

The emerging Urban Air Mobility (UAM) industry is generating significant levels of interest for aircraft designers, manufacturers, consumers and enthusiasts though the development of new electric Vertical Take-off and Landing (eVTOL) vehicles. The goal for the industry is to change the paradigm for personal transportation using these new types of vehicle operating under an entirely new set of rules in entirely new environments. There are a significant number of vehicle manufacturers (OEMs) designing and developing numerous types of eVTOL vehicles, and while the industry is in its infancy, there are many vehicle designs that are showing promise to achieve this goal.

The market is in rapid development and test flights on prototype eVTOL vehicles are scheduled to begin within the next few years. A review of information from manufacturer's websites and other publically available sources reveals there are some common traits many of these vehicles share. Typically, vehicles are configured to seat between 2 and 15 people and operate to varying degrees of autonomy within an urban environment. Common design features include redundant rotors or engines, distributed electrical power systems, and sensors for achieving autonomy. Furthermore, many of the OEMs are constructing vehicles out of advanced materials including carbon fiber composites in order to save weight and maximize efficiency.

The use of carbon fiber composite materials creates a significant weight reduction when substituted for traditional metallic materials. However, there are differences in the structural characteristics between metallic and composite materials. One of the major structural differences between the two material systems is, unlike metallic materials which exhibit ductility and plasticity, typical carbon fiber composites exhibit little ductility before ultimate failure. Vehicle designs using these materials must take into account these fundamental differences in material characteristics and must include features that take advantage of the properties that carbon fiber composites exhibit.

Perhaps the most important factor when considering the use of carbon fiber composites is the effect these materials will have on overall vehicle safety. While official Federal Aviation Administration (FAA) regulations on levels of safety have not been published as of the time of this writing, there needs to be a level of safety that will ensure widespread acceptance from the public who will be the eventual end users of these products. Guidance on design can be obtained from both current aircraft safety systems and also from the automotive industry. In an off-nominal event, such as a hard landing or crash, an injury mitigation system needs to be present to reduce the levels of loading into the occupant. In the automotive industry, items such as crumple zones, seat bolsters, airbags, and seat belts have been developed, and are present to absorb the energy of an impact event and keep the occupant loads to sub-injurious levels. These systems, having been improved over the years, have worked extremely well to reduce the number of automotive fatalities, with one metric showing a reduction of fatalities by a factor of three between 1975 and 2010 [1]. The design of eVTOL vehicles will require similar focus on the material systems and components used to achieve a similar assurance of safety.

This report will focus on one of the components that can be used to attenuate impact loading in order to achieve a higher level of safety - the landing gear. Various designs of energy absorbing landing gear systems exist currently with one of the most widely-used designs being the oleo strut. This strut design contains two chambers of damping liquid (typically oil and air) which are coordinated to dampen vibrations and lessen the acceleration loads upon landing. Many General Aviation (GA) aircraft and almost all major transport aircraft use some form of the oleo strut. A second, more fundamental, landing gear design is a spring steel strut that is configured to deflect, similar to the way a leaf spring deflects, upon aircraft landing to absorb the landing loads. These designs are popular with older light aircraft and are used because of their simplicity.

Both the oleo and spring steel struts, however, bear significant weight costs that may preclude them from being used in advanced lightweight composite vehicles. Many conceptual eVTOL vehicles appear to use a carbon-fiber rigid landing gear. While the design characteristics of each vehicle's landing gear system are unknown at present, much is known about the carbon fiber material itself and its failure characteristics. There have been many studies on the failure characteristics of crushable carbon structures [2-4], some of which include a tube/cylindrical design.

However, a new approach will be described in this report which seeks to create a controlled and repeatable crush mode that defines the failure using plastic deformation of a hybrid composite material system. The gear, as a part of a systems level approach to vehicle safety, could be the first line of defense in reducing the crash loads to sub-injurious levels.

Finally, when examining components using composite materials, the manufacturability of the design needs to be addressed. Manufacturability refers to the development of components that can be mass-produced without undue constraints that make them cost or time prohibitive. The UAM industry would ideally operate closer to the automotive business model where mass production and large number of vehicles can be assembled per year, rather than an aerospace business model were the mass production of aircraft means the manufacture of less than 700 per year [5]. The takeaway is that a design for a system or component on a mass produced vehicle must be lightweight, simple, and inexpensive.

Material Background

There are hybrid composite material systems that exist that combine the features of a carbon fiber system with the ductility of a metallic system. NASA LaRC has investigated these systems for use in previous energy absorbing applications [6-7] and has determined that they may hold promise for the development of a crushable landing gear component.

Hybrid composite material systems consist of a combination of carbon and non-carbon fibers in a woven layup configuration. The carbon fibers typically are oriented in the warp direction while the non-carbon fibers are oriented in the fill direction. Accordingly, the directionality of the fibers gives the finished material orthotropic material properties. By designing to and optimizing the orthotropic nature of the material, desirable characteristics in both material stiffness and compliance can be achieved. Figure 1 shows a close-up of a hybrid material system. The darker carbon fibers are oriented vertically, while the non-carbon fibers are oriented horizontally.
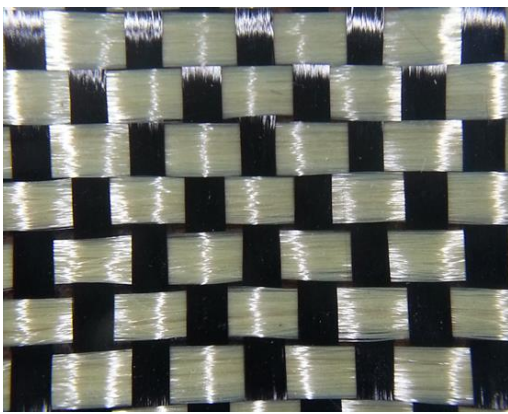

Figure 1 - Hybrid composite material system

Three material systems were examined at NASA LaRC for their potential use in a landing gear application. The first was a traditional carbon plain weave, designated as C/C, which has 3k-sized carbon tows in both the warp and fill directions, and was used more as a control rather than a crushable design material selection. The second was a hybrid material, which consisted of plain weave 3k-sized carbon fibers in the warp direction and 3k-sized aramid fibers in the fill direction. This material system will be designated as C/A. The third was a hybrid material system, which

consisted of twill weave of 3k-sized carbon fiber in the warp direction and 3k, sized ultra-high molecular weight polyethylene (UHMWPE) material in the fill direction. This material system will be designated as C/U. A twill weave system was used for the C/U material system since a plain weave system was not available.

Material property tests were performed to gain an understanding of the general strengths and stiffness characteristics of the material systems, as well as to determine their bounds. Four-layered panels were manufactured using hand lay-up techniques and cured under a vacuum at room temperature for 24 hours. Specimens were then cut out of the panels and all material tests were performed in accordance to ASTM 3039 [8] for the warp and fill directions and ASTM 3518 [9] for a 45° orientation to obtain shear properties. A full set of material properties was obtained in 2014 [6], and is reprinted in Table 1.

Table 1 - Material Properties

	Modulus (Msi)	**Ult. Strength (ksi)**	**Ult. Strain (in./in.)**
Warp Direction			
C/C	6.5	76.3	0.011
C/A	6.3	77	0.013
C/U	5.4	56	0.011
Fill Direction			
C/C	6.5	76.2	0.011
C/A	2.8	54	0.025
C/U	2.6	67	0.033
45° Direction			
C/C	0.79	17.4	0.20
C/A	0.45	3.1	0.45
C/U	0.33	8.3	0.15

All three material systems contained the same amount of carbon fibers in the warp direction, and the data shows that the modulus, strength and ultimate strain are very similar for the C/C and C/A material systems. The C/U material system shows slightly lower values in the modulus and strength categories, suggesting that the interaction between the carbon and UHMWPE fibers may be a factor in this material system. In the fill direction, the C/C specimens showed repeatable

results, while the C/A and C/U material systems exhibited a significant reduction in both modulus values and strength. However, what the materials lost in strength, they gained in an increased ultimate strain value. It was in the fill direction that the hybrid material systems exhibited the ductility from the non-carbon fibers. In the shear direction, all specimens exhibited significant reductions in the modulus and strength parameters. The smallest reduction was in the C/C strength parameter, with the 45° reduced by a factor of 4.3. The largest difference was exhibited by the C/A material system. The material strength when going between the warp direction and the 45° direction was reduced by a factor of approximately 25. However, the ultimate strain for all material systems was an order of magnitude higher when examining the 45° results, with the highest value occurring in the C/A material system at approximately 45% ultimate strain. The general trends obtained in the material property selection suggested that that C/C material system was the strongest but most brittle, while the C/A material system exhibited a strong but brittle warp direction and weak but ductile fill direction. The C/U material system was not as well defined, having a weaker warp direction but a stronger fill direction with a very small ultimate strain of 15%. The C/U material property results suggested complex fiber and/or material direction interactions may have been occurring and the results from further testing may depend on factors not yet realized. Furthermore, since the C/U material system was in a twill weave, the ratio of carbon to UHMWPE fiber was different than the C/C and C/A material systems, which were plain weave systems.

Once coupon material property data were obtained, the fabrication of the tubular specimens began. The specimen geometry was chosen to be 3 inches in diameter and 6 inches in length. These dimensions were chosen because they were able to be fabricated using methods and tools available, while also being within the family of sizes that could be used on eventual eVTOL vehicle landing gear designs.

Tube specimens were fabricated in-house at NASA LaRC using hand wet-layup techniques. The process involved first cutting the fabric material into a rectangular piece approximately 40 inches long by 7 inches tall. The rectangle was flattened, and the process of applying a wet layup of epoxy began. The wetted material was wrapped around a solid center core thus forcing the composite to cure in a tubular shape. The length of the rectangle allowed for four wraps around the center core, leading to a four layer composite wall design with a thickness of approximately 0.04 inches. The specimens were then set to cure at room temperature overnight. After cure, the core was removed, the specimen was cut to a 6 inch height and leftover material was discarded. To interface with the test machines, the specimens were potted into a rigid metallic base. Figure 2 shows examples of two fully cured completed composite tube specimens.

Figure 2 - Composite tube specimens. Traditional C/C (left), and C/A hybrid (right)

For a subset of tests, a 2.0 lb./ft.^{3} closed cell polyisocyanurate foam was used as the center core of the specimens. For these tests, the foam replaced the solid core and remained post-cure to become part of the final specimen design. Further investigations on the foam core included cutting either a 1-inch or 2-inch diameter hole leaving a partial core and void in the center of the specimen. The rationale behind including a foam core in its variations was to study its effect on crush strength behavior (if any), and to see if the foam would provide some stability during the crush event with particular emphasis focused in the off-axis loading condition. Figure 3 shows example specimens with the inclusion of the foam core. The solid core is shown on the left, the 1-inch diameter hollowed out core is in the middle, and the 2-inch diameter hollowed out core is on the right.
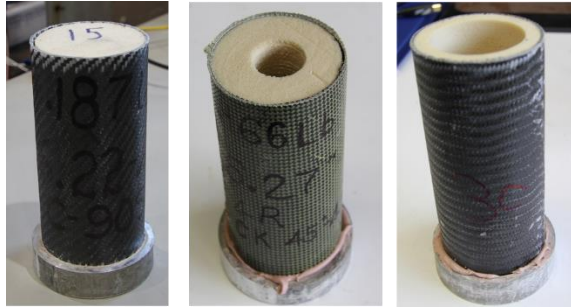
Figure 3 - Specimens with a foam core addition

Items such as fiber orientation and number of fiber layers were additional design variables that were initially considered and tested on a handful of preliminary specimens. However, previous data [6] demonstrated that layups of ±45° in hybrid material systems resulted in controlled crush of the specimens with highly uniform and predictable crush load, and the specimen results reported reflect this fabric orientation.

Final weights of the specimens were close in range. The hollow specimens ranged between 0.128 lb. for the C/C material system, 0.131 lb. for the C/A material system, and 0.163 lb. for the C/U material system. The C/C and C/A materials were similar, however the different twill weave configuration accounted for the added weight in the C/U material system. The addition of the foam core increased the weight by 0.05 lb., which was between a 30 to 38% increase, depending on the material system.

Test Results

The ultimate goal of the test program was to design a specimen capable of achieving less than a 20 g sustained crush acceleration through a stable crush pattern. After a series of material coupon tests, the tube specimens were evaluated under both static and dynamic conditions for impact energy attenuation characteristics and crush stability.

Static results

Specimens were first tested using a quasi-static loading rate of 0.25 in./min. Tests were conducted on specimens from each material system containing both a hollow core with no foam and with a fully filled foam core, to determine the effect (if any) of the foam on the crush response. Each test was stopped once the specimen achieved a quasi-uniform post-crush response, which for all specimens was greater than 25% strain. Table 2 shows a summary of the static data.

Table 2 - Static Test Data Summary

Material	Initial stiffness (klb./in.)	Crush initiation load (lb.)	Average post-crush sustained load (lb.)
C/C	41.4	4,175	1,157
C/C w foam	41.1	5,378	1,381
C/A	34.9	3,481	1,220
C/A w foam	35.1	3,343	1,509
C/U	21.7	2,082	1,441
C/U w foam	26.3	2,573	1,373

The stiffness result shown in Table 2 was calculated using the slope of the data occurring between the start of loading and 0.1 inches of displacement, which amounts to approximately 1.7% relative displacement for a 6-inch tall specimen. The C/C material system exhibited the highest initial stiffness of all the material systems. This result was not unexpected when comparing the trends to the material test results shown in Table 1, noting the C/C material system had the highest modulus is both directions. The C/A material system exhibited the second highest stiffness of 34.9 kip/in. while the C/U material system exhibited a comparatively significant drop in stiffness, at 21.7 kip/in.

The foam addition did not significantly change the results for either the C/C or C/A material systems. The C/C material system showed a slight decrease, while the C/A material system showed a slight increase in the initial stiffness. The decrease in stiffness is unexpected, and this result suggested that specimen-to-specimen variations resulting from the manufacturing process potentially played a role in specimen response. Only the C/U material system

showed a significant increase in stiffness of approximately 25%.

Similar trends appeared when examining the crush initiation load. The C/C material system exhibited the highest crush initiation loads, which were approximately 700 lb. higher than the C/A material system and almost 2000 lb. higher than the C/U material system. The C/C material system exhibited the highest crush initiation loads both with and without the foam core. The second highest crush initiation load was the C/A material system. The C/U material system exhibited the lowest crush initiation load. Sustained crush loads showed non-uniformities, which were attributed to defects in the manufacturing, but were similar when comparing averages using data between 5% and 16%, which corresponded to between 0.3 and 1 inches of crush displacement.

The foam played a differing role in all three material systems. For the C/C system, it raised both the crush initiation load and the post-crush sustained load. In the C/A system, it actually lowered the crush initiation load, but raised the post-crush sustained load, and achieved the opposite for the C/U material system. In the C/U material system, it raised the crush initiation load, but lowered the post-crush sustained load.

Some of the inconsistencies in the static results can be explained by recognizing that there was an unknown influence between the foam and the fibers in the material systems. A second source of the inconsistencies may also be attributed to the manufacturing process itself, with variations in cure time and laboratory conditions or other layup procedures playing a role in the results obtained. Further investigations into the strain fields that develop as the specimens reach the crush initiation load and also post-crush sustained load in the specimen walls may be required.

However, the values obtained from the static results show that either of the two hybrid composite material systems are suitable for a landing gear application. If a eVTOL vehicle were assumed to contain four struts, then the total crush initiation load for the C/A material system without foam would be 13,924 lb. If a total vehicle weight is assumed to be somewhere between 2,000 and 5,000 lb. - which is a realistic assumption

using weights from existing light aircraft - then the C/A strut design would withstand a hard landing or crash deceleration load of between 2.8 and 6.9 g, before initializing crushing. While 2.8 g may ultimately be too low of a threshold, the specimens are within the desired range.

The other notable difference was in the way the specimens exhibited failure. The C/C specimens exhibited a brittle fracture in the specimen walls, leading to a wall collapse. The C/A and the C/U specimens both exhibited a distinctive folding pattern of the cell walls, which contrasted the C/C behavior. The folding was progressive in nature, which led to the post-crush response having generally higher crush loads for the C/A and C/U specimens. Figure 4 shows a comparison of C/C and C/U specimens during the post-crush behavior. The C/C exhibited a fracture of the cell walls in the approximate middle of the specimen, while the C/U cell walls folded near the bottom of the specimen.
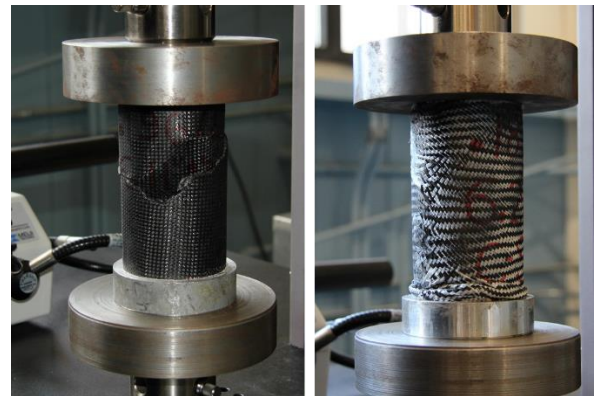

Figure 4 - Static test failure shapes. C/C (left) and C/U (right)

With static results showing the hybrid material systems generally providing a slightly better performance over the pure carbon system, a series of dynamic tests to evaluate the dynamic properties of the various combinations was performed.

Dynamic results

The vertical dynamic test setup consisted of an instrumented drop mass impacting a test specimen under a vertical drop tower at NASA LaRC. In all cases, a mass of 102 lb. was dropped from a distance of 6 feet, giving an impact velocity of approximately 19.6 ft./s. The mass initiated contact with the top of the specimen while the bottom of the specimen was fixed to a rigid base plate. A 500-g accelerometer, attached to the top of the drop mass, recorded the impact deceleration at 10 kHz. A high-speed camera was also recording the impact sequence at 1 kHz. Figure 5 shows the test setup.
.
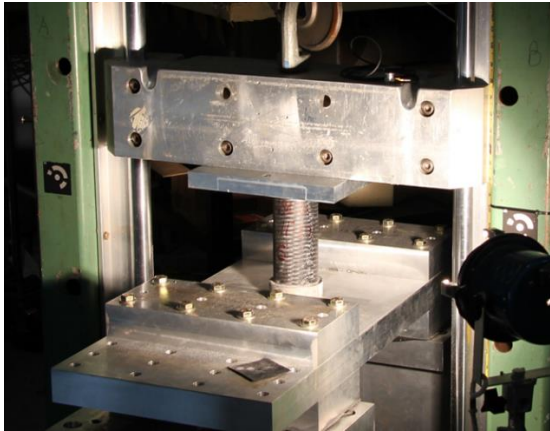
Figure 5 - Dynamic test setup

Maximum crush displacement was determined by examining the drop mass motion from the high-speed video data. The maximum distance the drop mass travelled after making first contact with the top of the specimen was reported as the crush distance. In many of the C/A and C/U specimens, there was a significant rebound of the mass after the maximum crush distance was achieved, indicating elastic qualities of the materials.

Figure 6 shows two frames of the high-speed video during a C/A material test. The frame on the left signifies the first observed fold in the material after drop mass contact, while the frame on the right shows the material as it sits at maximum mass displacement. The folding of the specimen walls are noticeable in the response of the specimen, as illustrated in Figure 6, right, and indicates the specimen exhibited this folding mechanism in both the static and dynamic material response beyond the crush initiation load.
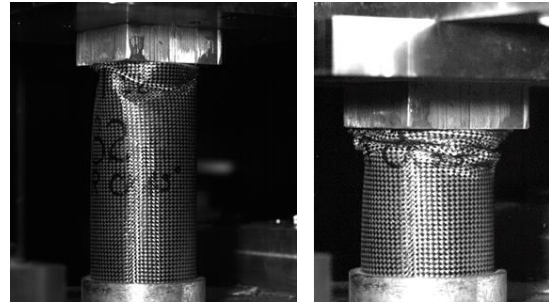

Figure 6 - C/A dynamic crush response. Crush/fold initiation (left) and maximum crush displacement (right)

The crush displacement for the C/A material system was 3.8 in. or approximately 63% of the specimen height. The number of folds was approximately 4 or 5. The acceleration from the falling mass was examined, and is shown in Figure 7. All acceleration values reported in this report were filtered with a 4-pole, low-pass, Butterworth filter with cutoff frequency of 1 kHz.
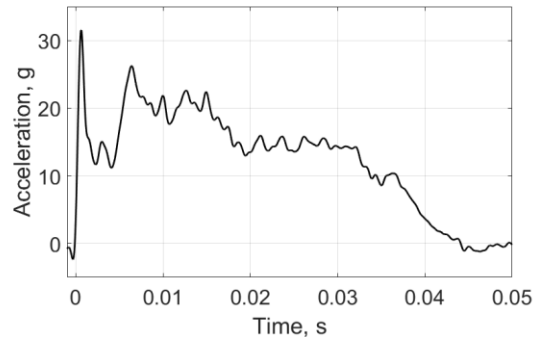

Figure 7 - C/A crush acceleration response

The initial crush initiation value in the response was 31.4 g, which occurred immediately after initial contact between the drop mass and the test specimen. It is important to note that "triggering mechanisms," or intentional defects manufactured into the specimen design in order to minimize this value were not included because the value of the initial load was considered an important data point to obtain. If required, a trigger mechanism can be incorporated into future designs and tested.

Beyond this initial load, the acceleration response settled into a post-crush sustained plateau of approximately 16.9 g. The plateau ran between 0.0022 s, which was the time of the first local

minimum after crush-initiation acceleration, and 0.032 s, the end of the sustained acceleration plateau.

The uniformity of the crush response during the plateau region was highly desirable as it indicated that the folding characteristics of the material system are capable of sustaining an approximate uniform value. The examination of the video data suggests the cause for the slightly higher area of acceleration between 0.005 and 0.015 s is due to a second fold initiation in the specimen walls. Since folds have already developed from the initial mass contact (Figure 6, left) additional values from fold initiation do not spike to as high of values.

Similar traits were exhibited for the C/U system. The post-crush folding behavior was present, however, folding began at the base of the specimen rather than at the point of drop mass contact. Figure 8 shows the C/U response, with folds at the base of the specimen.
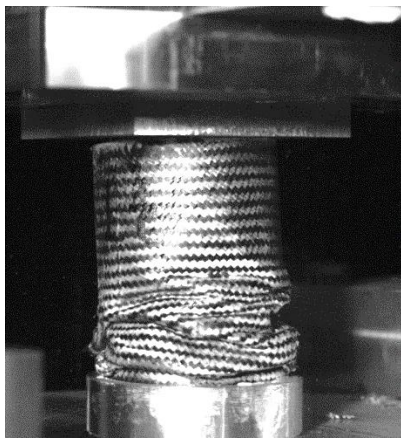

Figure 8 - C/U crush response

The number of folds was 4 or 5 and was similar to the C/A material. The maximum crush displacement was also similar to the C/A material system at 4.1 inches, and also exhibited some elastic rebound of the mass after maximum crush. The rebound was present due to the elastic characteristics of the non-carbon fibers for both the C/A and C/U material systems. The acceleration from the falling mass is next shown in Figure 9.
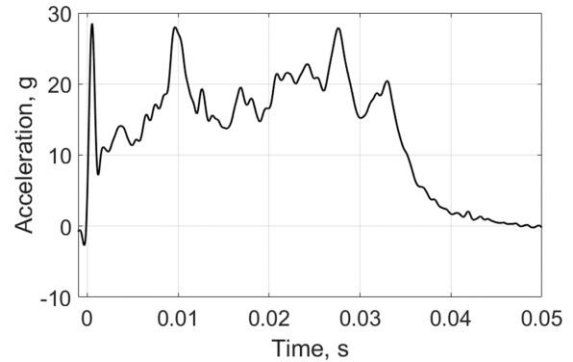

Figure 9 - C/U crush acceleration response

The C/U system exhibited a "choppy" plateau after the crush initiation value of 28.5 g. Additional spikes of 28 g and 27.9 g occurred at 0.0096 s and 0.028 s, respectively. Examination of the video offers no conclusive observation as to their root cause. Computing the average of the plateau between 0.0012 and 0.033 s. gives an average acceleration of 17.9 g, approximately 1 g higher than in the C/A material system.

Both of these responses were unlike the C/C system, which demonstrated catastrophic failure due to fiber pulverization upon drop mass contact with the specimen. With no ductile fibers to constrain the failures in the carbon fibers, the entire specimen peeled apart upon mass impact. Figure 10 shows the specimen response at maximum crush displacement.
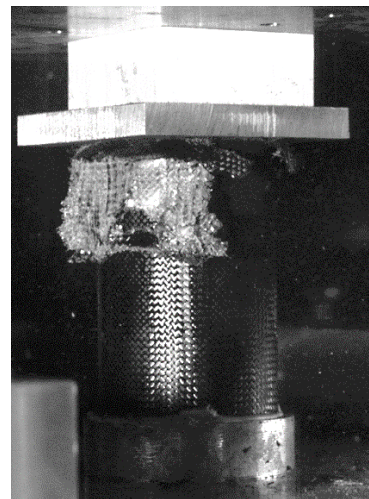

Figure 10 - C/C crush response

The acceleration response was significantly higher for the C/C specimen than for either the C/A or the C/U specimens. The initial crush initiation value was 46.4 g and a post-crush average acceleration was 28.2 g, which was approximately 10 g higher than either the C/A or C/U material systems. Figure 11 shows the measured acceleration from the C/C material system.
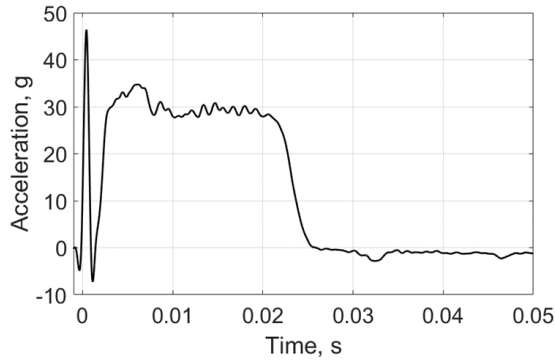

Figure 11 - C/C crush acceleration response

The specimens containing the foam core either fully solid or partially hollowed out behaved similarly to the non-core specimens presented. Both the C/A and C/U specimens still exhibited folding in the cell walls; however, the addition of the foam core increased the average crush response in most cases. Figure 12 shows results from specimens containing a solid foam core.
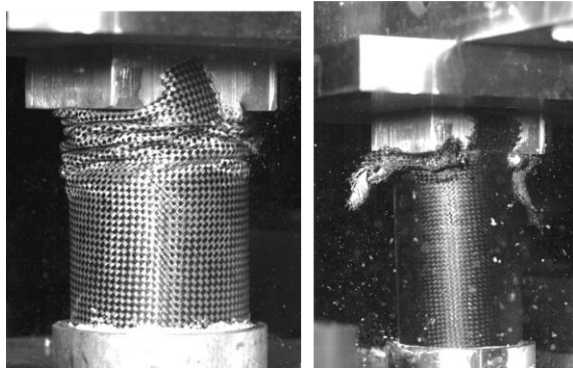

Figure 12 – Full foam core C/A (left) and C/C (right) crush responses

The C/A specimen is shown on the left with the folding of the cell walls clearly visible at the top of the specimen. While not specifically counted, the number of folds in the cell walls appears to be approximately 4 or 5, which was consistent with the other specimen results. The maximum crush displacement for the specimen was 3.2 inches, which was less than the 3.8 inches noted from the hollow C/A specimen behavior.

Following the trends of the C/A specimens, the addition of the foam in the C/C specimen decreased the maximum crush distance. The C/C with foam core maximum crush displacement was approximately 1.9 inches, compared to the 2.6 inches obtained from the hollow C/C specimens. In general, the decrease in the crush displacement is a function of the addition of the foam core.

Results for the various material systems are summarized in Table 3. Test #'s correspond to a larger test matrix, and are not necessarily in order by test performed. Specimens are listed in order according to the amount of foam present, from no foam to full foam, for each material system.

Table 3 - Dynamic Crush Results

Test #	Material	Average Acceleration (g)	Crush Displacement (in.)
C/C Material System			
33	C/C	28.2	2.6
36	C/C foam 2 inch	15.6	3.5
35	C/C foam 1 inch	32.4	2.1
14	C/C foam	37.1	1.9
C/A Material System			
17	C/A	16.9	3.8
28	C/A foam 2 inch	20.2	3.2
25	C/A foam 1 inch	22.8	3.0
8	C/A foam	23.5	3.2
C/U Material System			
20	C/U	17.9	4.1
27	C/U foam 2 inch	30.6	2.2
26	C/U foam 1 inch	34.0	1.9
13	C/U foam	17.0	4.3

A number of significant results are presented in Table 3. For the C/C material system, Test 36 fell out of family with the other C/C specimen results. Excluding this test, the data trended toward increasing crush load with decreasing crush displacement resulting from the

increased additions of the foam core. Further examination of Test 36 demonstrated that this specimen exhibited complete collapse of the specimen wall, similar to the static test results, and unlike other dynamic tests in which fiber wall peeling behavior was observed. The cell wall collapse is an indication of an unstable behavior which led to an increased crush displacement with decreased crush load. Because this type of failure response can exist in the C/C specimens, the C/C specimens were not determined to be suitable for further use in an energy absorbing landing gear strut design. Figure 13 shows a frame of high-speed video obtained during failure of the specimen in Test 36. The cell wall collapse is visible in the lower left side of the specimen.
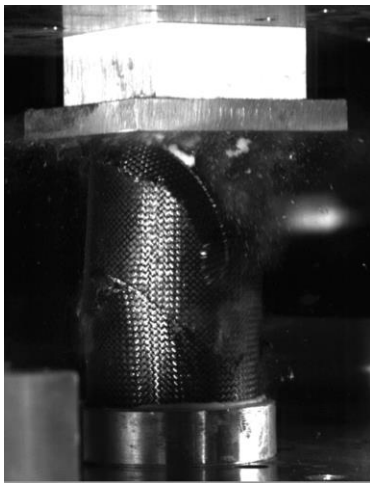

Figure 13 - C/C with 2-inch foam specimen crush response

The C/A material system was the most consistent of the three material systems tested. The addition of increasing amounts of the foam led to a steadily increasing crush load trend, with mostly decreasing crush displacement. The full foam cored specimen did show a slightly larger displacement than the 1-inch hollowed specimen, suggesting specimen-to-specimen variation. The consistency and repeatability of the C/A material response as a whole made it a prime candidate for further investigations both in test and analysis efforts.

Contrasting the C/A results, the C/U material system was the most inconsistent of the three material systems. The results for the C/U specimen with no foam core and the C/U specimen with a fully filled

foam core exhibited similar crush responses of 17.9 g and 17.0 g, and crushed a total of 4.1 inches and 4.3 inches, respectively. Conversely, the two specimens that contained the hollowed out foam exhibited high crush responses and little crush displacement. Other factors, which have been previously described, may have played a factor in the inconsistent results.

Without predictably, efforts to further evaluate the C/U material system were constrained so there were no further attempts at creating simulations on this material system. Instead, the simulation efforts focused on the traditional C/C and the hybrid C/A material systems.

Simulation Results

A commercially available, explicit finite element code, LS-DYNA® [10], was used to simulate each of the dynamic crush tests performed on the C/C and C/A materials. Simulations were carried out in order to determine the ability of computational models to replicate the failure characteristics of each material system; the patterns of brittle fractures for the C/C and the plastic folding for the C/A, as well as the prediction the energy dissipation characteristics of these crush tube designs.

The baseline model contained 11,174 nodes, 800 shell elements, and 8200 solid elements. The foam models with 2-inch, 1-inch, and no holes added an additional 2,400, 5,600 and 4,400 elements, respectively. The impactor was modeled as a solid rigid plate with equal mass to that used in testing. An initial velocity was applied to the impactor matching the test velocity at impact. An automatic single surface definition was applied between all parts. A single point constraint (SPC) was used to fix the bottom edge of the tube section in space.
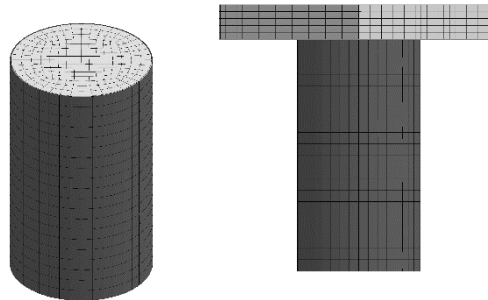
Figure 14 shows a depiction of the LS-DYNA simulation setup. All models were simulated to a termination time of 60 ms. Simulations were executed using LS-DYNA® SMP version R10.1.0 on a Linux-based cluster using 1 CPU with an approximate run time of 7 minutes without foam and 1 hour with foam.
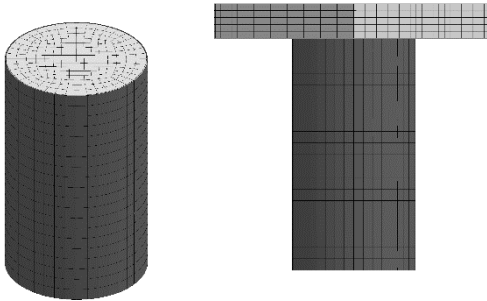

Figure 14 – Tube with foam core (left) and full setup (right) LS-DYNA simulation model

A small sensitivity analysis was performed on the shell element formation methodology. Fully integrated shell formulation was first attempted, but results showed that this formulation led to a significant over-prediction of initial impact acceleration, as well as increased oscillations during crush response. Thus the tubular composite sections were modeled using Hughes-Liu (single point integration) shell elements with viscous hourglass control. Each ply layer orientation, thickness, and material designation were defined using the *PART_COMPOSITE definition card. Previously developed and verified [7] Mat-58 (*MAT_LAMINATED_COMPOSITE_FABRIC) material model definitions for the C/C and C/A materials were used, and are reproduced in Table 4.

Table 4- LS-DYNA Material Property Inputs

	C/C Material	C/A Material
RO, lb.-s^2/in.^{2}	1.29E-4	1.29E-4
EA, psi	6.3E+6	6.3E+6
EB, psi	6.3E+6	2.76E+6
PRBA	0.1095	0.1095
TAU1, psi	4500.0	4500.0
GAMMA1, in/in	0.0246	0.0246
GAB, psi	3.0E+5	3.0E+5
SLIMT1	0.8	0.8
SLIMC1	1.0	1.0
SLIMT2	0.8	0.8
SLIMC2	1.0	1.0
SLIMS	1.0	1.0
AOPT	N/A*	N/A*
ERODS	0.5	0.5
FS	-1	-1
A1,A2,A3	N/A*	N/A*
D1,D2,D3	N/A*	N/A*
E11C, in/in	0.013	0.013
E11T, in/in	0.0143	0.0143
E22C, in/in	0.013	0.025
E22T, in/in	0.0143	0.025
GMS, in/in	0.142	0.142
XC, psi	70,000.0	70,000.0
XT, psi	89,000.0	89,000.0
YX, psi	70,000.0	50,000.0
YT, psi	89,000.0	54,000.0
SC, psi	7,100.0	7,100.0

*AOPT parameter not used as ply direction defined in PART_COMPOSITE.

The foam parts were modeled using constant-stress solid elements using material model Mat-63 (*MAT_CRUSHABLE_FOAM) with material properties previously developed for the foam [11]. A 0.01-inch offset was modeled between foam and composite tube, to allow a stable contact definition between the two parts.

A total of 16 unique test simulations were run, encompassing the various material, layup, and foam configurations tested. The simulations were first evaluated through qualitative examination of the crush patterns predicted by the C/C and C/A material models. This evaluation was completed to verify the models adequately captured the unique failure mechanisms of each material observed in testing. Figure 15 shows examples of predicted post-test crush response in the C/C material system on the left and the C/A material system on the right.
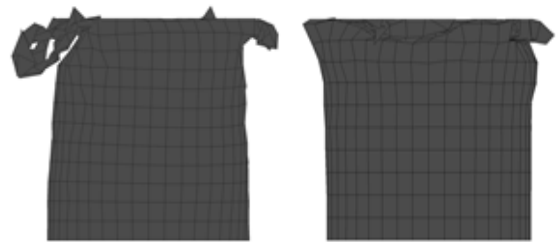
Figure 15 - C/C (left) and C/A (right) simulation results

The C/C model exhibited similar fiber break patterns to those seen in the test, with the specimen failing through vertical crack propagations in the material. The C/A material system exhibited the same distinct folding pattern as observed in test. The similarities in the failure shapes predicted gave confidence that the material definitions used. A comparison of acceleration time histories between the test and simulation results for the two identified material systems are shown in Figure 16.
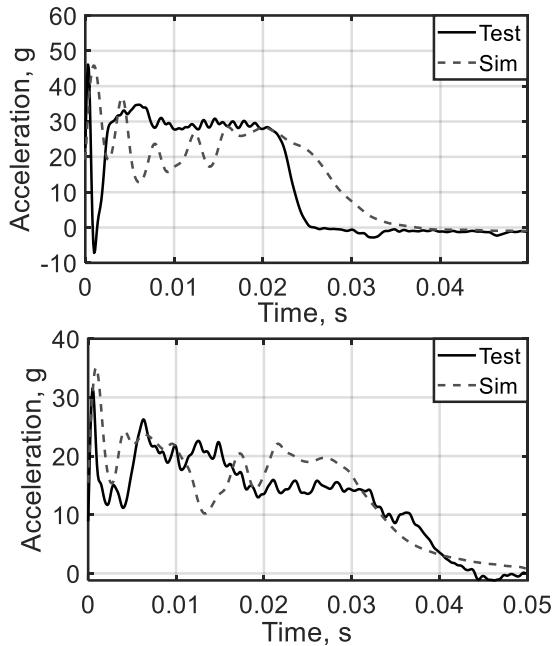

Figure 16 - Test to simulation acceleration comparisons, C/C (top) and C/A (bottom).

The C/C model closely predicted the initial acceleration from the impact into the specimen. During the beginning of the crush sequence the model under-predicted test acceleration, oscillating around 20 g. Towards the end of stable crush the model's prediction improved. After 0.025 s., test acceleration drops off steeply. Examination of the test videos revealed that at this time the carbon specimen exhibited unstable crush and buckling. The instability of the crush/buckling mechanism for this material caused late crush correlation to be difficult. The C/A model exhibited close correlation throughout the entire test period. Initial acceleration and following drop-off was closely predicted. During sustained crush, the simulation exhibited larger oscillations of

acceleration than test, but the general oscillation behavior was in line with the observed response from the test. The additional foam simulations exhibited similar correlation in both composite models. Figure 17 shows the C/A model.
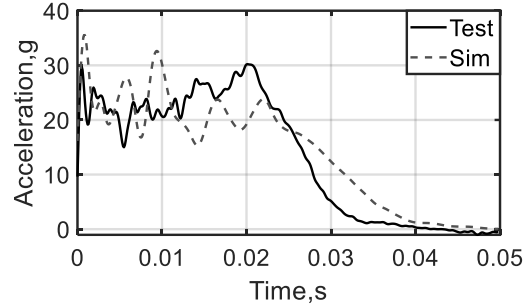

Figure 17 - Test to simulation acceleration comparison C/A with foam.

The foam addition was not shown to significantly change the correlation of either models. The addition did cause a slight increase in over prediction of the initial acceleration as well as the oscillations observed in simulation response. Similar effects were observed in the 1-inch hole simulations. The 2-inch hole had the opposite effect on initial impact correlation, resulting in an under prediction from the initial crush initiation.

To evaluate the developed C/A tube sections for use in a potential eVTOL vehicle design, off-axis loading was evaluated through an additional series of simulations using the developed material models and geometries. Simulations were performed with the tube sections constrained at 45°, 22.5°, and 10° to a drop mass of similar weight and velocity to that used in the vertical drop tests. Both ends of the tube were fixed with rotational joints that allowed it to rotate in plane with the impact load, as shown in Figure 18.
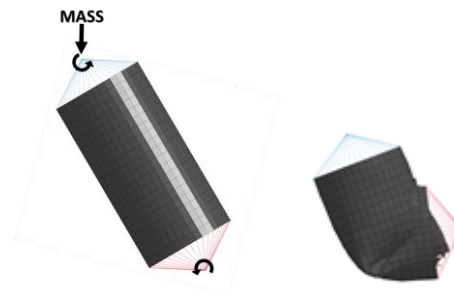
Figure 18 – Off-axis simulation setup (left) and post impact (right)

Simulations of the tubular sections exhibited buckling in all off-axis loading conditions. This buckling behavior resulted in complete failure of the system with minimal energy dissipation. In order to develop a tubular composite design which exhibits adequate energy absorption under vertical and off-axis loading, a design study to improve the tested tubular shape was carried out. Design alterations included edge and center diameter variations as well as ribbing within the tubular shape with variations on the spacing and uniformity of the ribs. An accordion like design with uniform 0.25-inch deep ribbing spaced 1.8 inches across the length, which is shown in Figure 19, was found to exhibit the most stable crush response under the 45°, 22.5°, and 10° loading conditions simulated. This design drives the tubular section to enter folding under off-axis load before it can buckle, resulting in controlled energy dissipation.
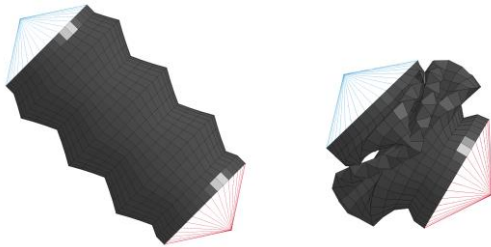

Figure 19 – Accordion crush tube design (left) and post impact (right)

With an understanding of and confidence gained in the simulation results, additional simulations were run varying geometric and material design parameters using a sample eVTOL vehicle in order to assess the feasibility and effectiveness of energy absorbing composite structures. The complete results, which are detailed in [12] are presented as an understanding of use of these systems in a realistic crash scenario with realistic vehicle parameters such as geometry, weight, and inertia.

Conclusion

The tests described in this report were used to gain an understanding of the fundamental behavior for three different material systems configured into a crush tube component. In a sense, the tests described were an initial effort to screen these material systems and as a first step toward eventual use in eVTOL vehicle applications. Each fabric was chosen due to its relatively low cost, ease of manufacturability, and material availability. A subset of specimens added a closed cell foam core to determine the effect on the crush loads and stability. The inclusion of the foam added weight to the original specimen design, so a subset of the foam specimens were hollowed out, leaving various sized cavities in their center.

Once basic material properties were generated, each material's crush parameters and failure characteristics in both static and dynamic regimes were obtained and evaluated against the others to determine whether one material system performed significantly better than the others. Several conclusions were drawn from the test series. The C/C material system showed both the highest initial stiffness along with the highest crush loads, and was the only material system that exhibited brittle failure characteristics. While in some tests, fiber splaying was the major mode of failure, leading to the highest sustained crush load, under certain tests, there was a catastrophic collapse of the cell walls, leading to a low sustained crush load and a large amount of crush displacement. The tests where the cell walls collapsed were unacceptable when characteristics such as uniform sustained crush loads and repeatable behavior are required. The general conclusion from the C/C material system was that it performed as anticipated – strong and brittle - with some of the test results suggesting an inconsistency in material response.

The C/A material system exhibited the greatest uniformity and repeatability in sustained crush behavior. In *all* tests, the C/A specimens exhibited a distinct cell wall folding characteristic leading to large generally uniform sustained crush loads. The initiation load was between that of the C/U and C/C material systems, and the results presented anticipate that the C/A material system would be well suited for applications needing a repeatable, predictable crush response. The component level test results demonstrate that the material could achieve a sustained loading level at around 20 g, with a high load initiation of short duration.

The C/U material system exhibited the greatest variability in the test results. In some of the tests, there

was a distinct folding characteristic like those seen in the C/A system, while in others there was catastrophic failure in the cell walls, like what was seen in the C/C material system. Further investigations are needed into the C/U material system to determine whether variability in results is influenced by cure time, cell wall thickness or other manufacturing or testing parameters that were present to influence the results.

Simulation efforts were able to capture the test behaviors for both the C/C and C/A material systems. The crush/failure mechanisms of both material systems were predicted by their respective material models. The acceleration response of the C/C model closely predicted crush initiation but did exhibit under-prediction of sustained acceleration during initial crush. The C/A material model closely predicted tests throughout the crush profile. It should be noted that during simulation development a sensitivity to shell formulation was identified. Fully integrated shell formulation led to a significant over-prediction of initial impact acceleration, as well as increased oscillations during crush response. The decision was made to go to a single-point Hughes-Liu element with hourglass control. It is postulated that the Hughes-Liu produced better correlation because the original material models were developed using a single point integration formulation. With this in mind, the results of this study do lend confidence in using both of these material models with this shell element formulation to accurately predict the response of their physical counterparts.

Simulations into variations in the C/A specimen geometry were run in order to determine an optimal design for an off-axis crushing event. The simulations varied the cell wall diameter along with the length of the tube section in order to achieve a stable result without too high of a sustained crush load. A suitable design that resembled an accordion was developed, which exhibited the desired crush response for this system. Further testing must be completed in order to fully assess this design.

While the specimens documented in this report are only a first step in achieving what could be a new energy absorbing strut design, there are many design variable that are available for use to create a lighter, safer, eVTOL vehicle. Items such as landing gear

struts, energy absorbing subfloors, seats and restraints all should be used in harmony to achieve increased safety levels for occupants. It is only through these increased safety features that there will be widespread acceptance of these vehicles by the public for this new and burgeoning industry.

References

1. Glassbrenner, D. "An Analysis of Recent Improvements to Vehicle Safety." DOT HS 811 572. June 2012.

2. Deleo, F., Wade, B., Feraboli, P., and Rassaian, M. "Crushing of composite Structures: experiment and simulation." 50th AIAA/ASME/ASCE/AHS/ASC Structures, Structural Dynamics and Materials Conference. Palm Springs, CA. May 4-7, 2009.

3. Thorton, P.H. and Edwards, P.J. "Energy Absorption in Composite Tubes." J. Composite Materials, Vol 16. P 521. November 1982.

4. Luo, H., Yan, Y., Meng, X., and Jin, C. "Progressive Failure Analysis and Energy-Absorbing Experiment of Composite Tubes Under Axial Dynamic Impact." Composites Part B: Engineering. Vol. 87, Pp 1-11. February 2016.

5. Adams, E. "The Need for Carbon Fiber Could Ground the Flying-Car Future." Wired magazine. https://www.wired.com/story/air-taxi-flying-cars-carbon-fiber-production-icon-a5/ January 29, 2019.

6. Littell, J.D. "The Development of a Conical Composite Energy Absorber for use in the Attenuation of Crash/Impact Loads". Paper/presentation at the American Society of Composites 29th Annual Conference, San Diego CA. September 8-10 2014.

7. Jackson, K.E., Fasanella, E.L., and Littell, J.D. "Development of a Continuum Damage Mechanics Material Model of a Graphite-Kevlar ® Hybrid Fabric for Simulation the Impact Response of Energy Absorbing Subfloor

Concepts." Proceedings from the 73rd Annual American Helicopter Society Annual Forum and Technology Display. Fort Worth TX. May 9-11, 2017.

8. American Society for Testing and Materials. "Standard Test Method for Tensile Properties of Polymer Matrix Composite Materials." ASTM-D3039M. 2008.

9. American Society for Testing and Materials. "Standard Test Method for In-Plane Shear Response of Polymer Matrix Composite Materials by Tensile Test of a ±45° Composite." ASTM-D3518M. 2013.

10. LSTC. "LS-DYNA Theory Manual," Livermore Software Technology Company, Livermore, CA. July 2017.

11. Jackson, K.E., Fasanella, E.L., and Littell, J.D. "Impact Testing and Simulation of a Sinusoid Foam Sandwich Energy Absorber." Proceedings from the 30th American Society for Composites Technical Conference. East Lansing, MI. September 28-30, 2015.

12. Putnam, J.B. and Littell, J.D. "Evaluation of Impact Energy Attenuators and Composite Material Designs of a UAM VTOL Concept Vehicle." Proceedings from the 75th Vertical Flight Society Annual Forum and Technology Display. Philadelphia, PA. May 13-16, 2019.